SPECIAL ISSUE ARTICLE

Physiologia Plantarum

Leaf density and chemical composition explain variation in leaf mass area with spectral composition among 11 widespread forbs in a common garden

Qing-Wei Wang[1,2] | Chenggang Liu[3,4] | Thomas Matthew Robson[5] |
Kouki Hikosaka[6] | Hiroko Kurokawa[2]

[1]CAS Key Laboratory of Forest Ecology and Management, Institute of Applied Ecology, Chinese Academy of Sciences, Shenyang, China

[2]Department of Forest Vegetation, Forestry and Forest Products Research Institute, Tsukuba, Japan

[3]CAS Key Laboratory of Tropical Plant Resources and Sustainable Use, Xishuangbanna Tropical Botanical Garden, Chinese Academy of Sciences, Menglun, China

[4]Center for Plant Ecology, Core Botanical Gardens, Chinese Academy of Sciences, Xishuangbanna, China

[5]Organismal and Evolutionary Biology, Viikki Plant Science Centre (ViPS), University of Helsinki, Helsinki, Finland

[6]Graduate School of Life Sciences, Tohoku University, Sendai, Japan

Correspondence
Qing-Wei Wang, CAS Key Laboratory of Forest Ecology and Management, Institute of Applied Ecology, Chinese Academy of Sciences, Shenyang 110016, China.
Email: wangqingwei@iae.ac.cn and wangqw08@gmail.com

Abstract

Leaf mass per area (LMA) is a key leaf functional trait correlated with plant strategies dictating morphology, physiology, and biochemistry. Although sunlight is generally accepted as a dominant factor driving LMA, the contribution of each spectral region of sunlight in shaping LMA is poorly understood. In the present study, we grew 11 widespread forb species in a common garden and dissected the traits underpinning differences in LMA, such as its morphological components (leaf density [LD] and leaf thickness [LT]), macroelement, and metabolite composition under five spectral-attenuation treatments: (1) transmitting c. 95% of the whole solar spectrum (> 280 nm), (2) attenuating ultraviolet-B radiation (UV-B), (3) attenuating both UV-A and UV-B radiation, (4) attenuating UV radiation and blue light, (5) attenuating UV radiation, blue, and green light. We found that LMA, LD, and chemical traits varied significantly across species depending on spectral treatments. LMA was significantly increased by UV-B radiation and green light, while LD was increased by UV-A but decreased by blue light. LMA positively correlated with LD across treatments but was only weakly related to LT, suggesting that LD was a better determinate of LMA for this specific treatment. Regarding leaf elemental and metabolite composition, carbon, nitrogen, and total phenolics were all positively correlated with LMA, whereas lignin, non-structural carbohydrates, and soluble sugars had negative relationships with LMA. These trends imply a tradeoff between biomass allocation to structural and metabolically functional components. In conclusion, sunlight can spectrally drive LMA mainly through modifying functional and structural support.

698 | wileyonlinelibrary.com/journal/ppl   *Physiologia Plantarum.* 2021;173:698–708.

1 | INTRODUCTION

Plant functional traits generally reflect trade-offs in plant acquisition/investment according to the limiting resources in their environments (Wright et al., 2004). Leaf mass per area (LMA), as the key trait to the 'leaf economic spectrum (LES)', is an indicator of leaf physiological and morphological function (e.g., photosynthesis and defense) (Poorter et al., 2009; Poorter et al., 2019; Reich et al., 1997), as well as ecosystem properties and processes (e.g., primary productivity and litter decomposability) (Adler et al., 2014; Cornwell et al., 2008; Duursma & Falster, 2016; Wright et al., 2004). A better understanding of the abiotic drivers (e.g., light) of variations in LMA, and the structural and compositional basis of LMA, is required to improve our capacity to predict how ecosystem functioning responds to ongoing climate changes (e.g., cloudiness, aerosol pollutants, and forest fires).

LMA is determined by two structural components, leaf thickness (LT) and leaf density (LD, dry mass per unit volume): $LMA = LT \times LD$ (Poorter et al., 2009; Witkowski & Lamont, 1991). Increases in LT are primarily associated with additional mesophyll thickness (e.g., increase in the layers and volumetric fraction of palisade cells) (Coble & Cavaleri, 2017; Griffith et al., 2016; Niinemets, 1999). A higher LT can contribute to higher photosynthetic capacity under high light (Oguchi et al., 2005) or higher water use efficiency under drought conditions (Wright et al., 2002). Variation in LD is generally related to changes in mesophyll cell size, air spaces, and the volume fraction of the cell wall (Niinemets, 1999; Poorter et al., 2009). Tightly packed mesophyll cells with thickened cell walls would increase LD and constrain mesophyll conductance, limiting photosynthesis and carbon (C) uptake (John et al., 2017; Niinemets, 2001), but increase robustness against water loss and herbivory (Peeters, 2002). On the other hand, leaf nutrients or chemical compounds per unit leaf area are positively related to LD and LMA (Poorter et al., 2009; Poorter & Villar, 1997). For instance, LMA increases with a greater proportion of leaf C (de la Riva et al., 2016) and total non-structural carbohydrates (NSC) (Xu et al., 2012), and with low nitrogen (N) concentration (de la Riva et al., 2018). Therefore, the extent to which LMA responds to environmental changes strongly depends on its structural and functional basis.

A large number of studies focusing on the plasticity of LMA to abiotic factors have found that it responds to numerous changes in environmental conditions in nature; the factors driving variation in LMA include light (Coble & Cavaleri, 2015; Fajardo & Siefert, 2016), temperature (Fajardo & Piper, 2011; Zhang et al., 2020), water (Fernandez-Martinez et al., 2016; Sanchez-Gomez et al., 2013), nutrients (Onoda et al., 2008; Wang et al., 2019), and CO_2 (Hikosaka et al., 2005; Ishizaki et al., 2003). However, a meta-analysis from Poorter et al. (2009) has identified that light is the dominant factor driving LMA variation, exceeding temperature in importance, based on LMA data from a total of 3800 species across functional groups and ecosystems types. The positive correlation across species between irradiance and LMA suggests that plants may have strategically adapted to changes in light conditions to increase leaf area for light interception under low light and photosynthetic capacity under high light. Poorter et al. (2019) further generalized irradiance–response curves for 70 traits related to leaf morphology, chemistry, and physiology of 760 species: Plasticity in both LT and LD tended to double over the studied light range (0.2–75 mol m^{-2} d^{-1}), equally contributing to the 2.6-fold increase in LMA from low to high irradiance. Although previous meta-analyses provide a general picture of the response to light intensity (quantity), the related mechanisms behind these responses, particularly the extent to which such changes are determined by spectral composition, are less well described.

Sunlight does not only supply the essential energy input for photosynthesis (Hikosaka et al., 1994; Moss, 1967; Oguchi et al., 2017), but importantly provides cues that regulate leaf traits and dictate plant functional strategy (Ballaré, 2014; Jenkins et al., 2001; Wang et al., 2020). The incident solar radiation is composed of multiple spectral regions, which are important for plant function, from ultraviolet (UV)-B (280–315 nm) to red light (600–700 nm). Photoreceptors absorb specific spectral regions and are well documented to regulate a set of molecular, physiological, and biochemical processes (Casal & Qüesta, 2018; Robson et al., 2019; Smith et al., 2017; Verdaguer et al., 2017). Briefly, UV-B radiation (280–315 nm) and UV-A radiation below 350 nm sensed by UVR8 (UV RESISTANCE LOCUS8) can induce the synthesis of UV-absorbing compounds (e.g., phenolics) to attenuate excess UV-B radiation (Casati et al., 2011; Rai et al., 2019). Blue light (400–500 nm) increases LMA and leaf N concentration, and promotes photosynthetic efficiency (Hogewoning et al., 2010) through activating photoreceptors, cryptochromes (CRYs), phototropins (PHOTs), and proteins from the zeitlupe family (Casal, 2000; Lin, 2000). Red light (600–700 nm) decreases LMA, LT, N, and NSC concentrations (Hu et al., 2016; Liu et al., 2018) by activating phytochromes (PHYs) (Smith, 2000). Green light (500–600 nm) induces shading syndromes antagonistically to blue light (Smith et al., 2017). However, even though the roles of each spectral region have been explored in molecular biology and actively applied in horticulture (Brelsford et al., 2019; Hogewoning et al., 2010; O'Hara et al., 2019; Rai et al., 2019), the ecophysiology behind how these regions of sunlight interact to affect plant functional traits outdoors has not been entirely resolved, since multiple wavebands may coordinate leaf responses simultaneously through crosstalk among photoreceptors (Casal, 2000; Rai et al., 2019).

Although several ecological studies have focused on responses to changing UV-B radiation and red to far-red ratio (R/Fr) to respectively assess how plants acclimate to UV-B stress (Rousseaux et al., 2004; Searles et al., 2001) and shade (Aphalo & Lehto, 2001; Razzak et al., 2017), spectral regions from the photosynthetically active radiation (PAR) are not often included in such studies. In the present study, we assessed variation in LMA and components (both morphological and chemical) of 11 common forb species growing under spectral-attenuation-filter treatments. We aimed to answer the questions: (1) Which spectral regions determine LMA? (2) How does variation in LD and LT explain changes in LMA? (3) Is the change in LMA with spectral composition related to differences in leaf metabolic, structure, and elemental composition?

2 | MATERIALS AND METHODS

2.1 | Plant materials

The present study used 11 widespread light-demanding forb species (see species list in Table 1). Most species are sun plants, but some favors shade conditions. Seeds were collected from Tsukuba Botanical Garden, National Museum of Nature and Science, Tsukuba, Japan (36°00′N, 140°08′E). Seeds were sown on 25th May 2018 into pots with a volume of 438 cm^3 (9.0 × 7.6 × 6.4 cm) in a greenhouse of the Forestry and Forest Products Research Institute (FFPRI), Tsukuba, after vernalization on wet filter papers for 4 days at 4°C in the dark. The order of sowing seeds was opposite to the germination order, and the timing was controlled to ensure the initial age of seedlings was relatively homogenous across species. Pots were filled with a mixture of compost, including vermiculite, kanuma soil, and pumice [6:1:2:1(v/v)]. We watered pots from beneath through the trays every 3 days and supplied nutrients once per week with a commercial liquid fertilizer (N–P–K = 6–10–5%, HYPONEX, Japan). The nutrient dose was diluted to a concentration of 1.2 ml/L, 7.5 ml/pot. Dead individuals during the experimental period were removed.

2.2 | Experimental growth conditions

We carried out this spectral-attenuation experiment in a large unshaded garden at FFPRI. Details are described in a previous study (Wang et al., 2020). Briefly, we attached the plastic filters to 1.2 × 1.0 m wooden frames at around 20° inclination (facing south), with additional filter pieces on both the East and West sides of frames, in order to attenuate diffuse sunlight early and late in the day. Five spectral irradiance treatments included: (1) Full-spectrum treatment (transmitting λ >280 nm, i.e., all solar UV-B), with a fully transparent polythene film (0.05 mm thick, 3904CF; Okura), transmitting approximately 95% of the whole solar spectrum; (2) No-UVB treatment (λ >315 nm), attenuating UV-B radiation (0.125-mm-thick polyester film, Autostat CT5; Thermoplast); (3) No UV treatment (λ >400 nm), attenuating all UV radiation (0.2-mm-thick Rosco E-Color 226 filter, Westlighting); (4) No UV/Blue treatment (λ >500 nm), attenuating all UV and blue wavelengths (0.20-mm-thick Roscolux Supergel 312 filter); (5) No-UV and blue–green (UV/BG) treatment (λ >580 nm), attenuating all UV radiation and BG wavelengths (0.2-mm-thick Rosco E-Color 135 Deep Golden Amber filter) (Table 2).

Due to differences in transmittance ratios among filters, we added different types of spectrally neutral shade mesh below the filters, allowing seedlings to receive equivalent PAR irradiance across treatments. The average PAR under each frame was 14% of ambient sunlight (Table 2), determined by a quantum sensor (LI-190, Li-Cor Biosciences Inc). Attenuating solar radiation to create treatments at equivalent PAR irradiance allowed us to better distinguish spectral treatment effects rather than damage from high irradiance. The spectrum treatment created by each filter was determined under a clear sky at solar noon using a spectroradiometer (USR- 45DA; USHIO).

The spectral irradiance under each frame during the experiment was checked using a Maya 2000 Pro array spectrometer (Ocean Optics Inc.) calibrated for maximum spectral sensitivity in solar UV and PAR (Hartikainen et al., 2018).

The whole experiment was arranged in four randomized blocks of filters (in total 20 filter-frames), each block being a replicate (Figure S1). Twenty individuals of each species were randomly separated among the 20 filter-frames on June 23, 2018. Plants were placed in two plastic trays (51 × 31 × 5.3 cm) on a wooden shelf under the center of each frame to limit the diffuse solar radiation from outside. We changed filter height to keep them suspended around 20-cm above the upper leaves, and randomly rotated the position of the pots every week to ensure all seedlings grew in similar light conditions throughout the experiment. We supplied water twice a day (once at 8:00 a.m. and 7:00 p.m. for 60 s) using a purpose-built sprinkler system. Nutrients were supplied in the same way described above. Ambient PAR, UV-B, and UV-A radiation (Figure S2A,B) were measured and integrated over 15-min intervals using the LI-190SA sensor and two broadband UV-cosine sensors (UV-B and UV-A; sglux GmbH), respectively, with a data-logger (LI-1400; LI-COR). Air temperature approximately 20 cm above the pots (Figure S2C) was recorded at 30-min intervals using a HOBO H8 Pro temperature logger (Onset Computer Corporation, Bourne).

2.3 | Measurements of leaf traits

Fully expanded sun leaves (2–4 leaves per individual) were collected for chemical analysis under a clear-sky sunny day (August 27, 2018) at the end of the growing season. Leaf samples were ground into a fine powder after vacuum-drying (FDU–1200, EYELA) for 16 h. Leaf C and N concentrations were measured using an elemental analyzer (Vario MAX cube). The concentration of total phenolics was determined by the Folin–Ciocalteu method using tannic acid as a standard sample (Waterman & Mole, 1994). The concentration of lignin was measured by an improved acetyl-bromide procedure (Iiyama & Wallis, 1990) and calculated from the fitted calibration curve (Fukushima & Hatfield, 2001). The concentration of the condensed tannins was determined by a proanthocyanidin assay using cyanidin chloride as a standard sample (Julkunen-Tiitto, 1985). The concentrations of total soluble sugars and starch were determined using the anthrone method (Wang, Qi, et al., 2018). We defined NSC as the sum of total soluble sugars and starch. All chemical traits were expressed on a dry-matter basis (% dm) and an area basis (g m^{-2}).

Another equivalent pair of leaves were collected for measuring leaf morphological traits on August 28, 2018. Leaf area (LA, cm^2) was scanned and calculated with the Fiji software (Wang et al., 2020). LT (μm) was measured in four random places with a thickness gauge (model 547-401 m, 0.001 mm; Mitutoyo), avoiding both primary and secondary veins. The measured leaves were dried in an oven at 60°C for 48 h to obtain leaf dry mass (LM, g). LMA (g m^{-2}) was determined based on LA and LM of scanned leaves. LD (g cm^{-3}) was calculated from LM divided by LT and LA. Sampling was not done for two dead

TABLE 1 List of plant species and leaf traits in the common garden experiment and their functional classification

Traits	Adenophora triphylla var. japonica	Artemisia indica var. maximowiczii	Eupatorium japonicum	Eupatorium makinoi	Fallopia japonica	Geum aleppicum	Geum japonicum	Plantago asiatica	Platycodon grandiflorus	Prunella vulgaris subsp. asiatica	Senecio cannabifolius
LMA (g m^{-2})	30.6 (0.42)	22.7 (0.77)	23.8 (1.16)	37.3 (1.22)	26.7 (1.82)	23.2 (1.18)	37.5 (0.37)	49.8 (3.70)	39.7 (0.75)	24.0 (1.29)	28.8 (1.45)
LM (g)	0.15 (0.016)	0.03 (0.002)	0.10 (0.003)	0.24 (0.071)	0.06 (0.003)	0.06 (0.005)	0.30 (0.002)	0.09 (0.013)	0.19 (0.035)	0.03 (0.001)	0.04 (0.005)
LA (cm^2)	47.4 (4.82)	14.9 (0.69)	42.0 (2.21)	64.0 (16.97)	21.4 (2.71)	24.6 (3.05)	79.3 (0.49)	18.2 (3.16)	48.1 (9.12)	12.8 (0.75)	12.8 (1.56)
LT (um)	272 (4.79)	185 (6.45)	172 (14.4)	250 (20.0)	275 (25.0)	210 (15.8)	182 (8.00)	240 (14.1)	283 (9.46)	200 (18.7)	215 (16.6)
LD (g cm^{-3})	0.11 (0.001)	0.12 (0.003)	0.14 (0.006)	0.15 (0.007)	0.10 (0.002)	0.11 (0.011)	0.21 (0.008)	0.21 (0.02)	0.14 (0.006)	0.12 (0.01)	0.14 (0.010)
C (%)	42.9 (0.46)	43.5 (0.18)	42.6 (0.45)	41.3 (2.25)	41.1 (0.85)	44.0 (0.29)	42.2 (0.73)	37.2 (2.33)	40.1 (0.98)	42.6 (0.14)	43.2 (0.27)
N (%)	3.18 (0.19)	3.91 (0.06)	3.91 (0.14)	3.19 (0.08)	3.00 (0.22)	3.99 (0.09)	3.08 (0.27)	3.38 (0.13)	2.83 (0.16)	3.61 (0.03)	3.46 (0.20)
Phenolics (%)	4.76 (0.30)	5.51 (0.44)	1.63 (0.12)	2.29 (0.47)	8.31 (0.16)	2.53 (0.43)	13.9 (1.30)	10.53 (1.05)	2.46 (0.26)	3.77 (0.22)	1.45 (0.08)
Lignin (%)	6.63 (0.14)	5.62 (0.12)	4.39 (0.15)	5.31 (0.64)	5.10 (0.30)	4.01 (0.05)	6.51 (0.14)	7.04 (0.12)	5.88 (0.09)	6.05 (0.18)	3.93 (0.15)
Tannin (%)	0.94 (0.29)	0.13 (0.014)	0.13 (0.02)	0.19 (0.03)	0.19 (0.03)	0.15 (0.02)	0.18 (0.01)	0.16 (0.03)	0.17 (0.01)	0.20 (0.03)	0.16 (0.01)
NSCs (%)	6.16 (0.26)	12.0 (0.44)	5.76 (0.49)	6.61 (0.38)	9.24 (0.66)	5.89 (0.37)	10.9 (0.35)	12.17 (0.59)	7.29 (0.48)	5.13 (0.15)	12.9 (1.07)
Sugars (%)	3.11 (0.35)	9.26 (0.41)	4.12 (0.61)	4.29 (0.41)	5.18 (0.26)	3.34 (0.32)	7.99 (0.39)	8.35 (0.87)	4.18 (0.21)	2.42 (0.11)	7.26 (1.27)
Starch (%)	3.06 (0.36)	2.72 (0.24)	1.65 (0.12)	2.32 (0.28)	4.06 (0.40)	2.54 (0.44)	2.92 (0.22)	3.81 (0.71)	3.11 (0.41)	2.71 (0.18)	5.60 (0.56)

Note: Leaf traits of each species were measured from the full-spectral treatment (ambient sunlight group) at the end of the common garden experiment. Mean values (SE) are shown for each species (*n* = 11 replicates with one replicate being one plant and 1 measure per plant).

Abbreviations: C, carbon; LA, leaf area; LD, leaf density; LM, leaf mass; LMA, leaf mass per area; LT, leaf thickness; N, nitrogen; NSC, non-structural carbohydrates.

TABLE 2 Transmittance, spectral photon irradiances, and temperature under filters with shade meshes in the growth experiment. Values indicate means ($n = 4$)

Filters	Quantity (nm)	Transmittance (%)							Photon irradiances (μmol m^{-2} s^{-1})							Temp (°C)
		PAR	UV-B	UV-A	Blue	Green	Red	Far-red	PAR	UV-B	UV-A	Blue	Green	Red	Far-red	
Polythene	>280	14.0	10.1	12.5	13.5	13.9	14.3	14.8	231.5	0.4	17.6	45.8	56.6	52.3	39.8	29.1
Polyester	>315	13.4	0.0	8.8	12.8	13.4	13.8	14.3	302.2	0.0	16.2	58.6	74.2	69.2	52.5	29.6
Rosco 226	>400	13.6	0.2	1.3	13.1	13.8	14.2	14.4	261.0	0.0	2.0	50.7	64.6	60.2	45.3	29.5
Rosco 312	>500	14.9	0.1	0.7	0.9	17.0	22.1	22.9	287.6	0.0	1.1	3.5	80.0	94.4	72.6	29.3
Rosco 135	>580	12.5	0.0	0.3	0.3	0.8	29.4	32.1	238.9	0.0	0.4	1.1	3.7	125.3	101.1	29.2

Note: Filters were combined with different shade meshes to make light intensity similarly under all frames in the experiment. Measurements were done by A Maya 2000 Pro (Ocean Optics) spectrometer under each of the filters of July 23, 2018 at midday under a clear sky. Immediately after (within 2 min) each filter measurement, they were compared with the ambient solar spectral irradiance measured adjacent to the filter. Wavelength ranges in nm, PAR: 400–700; UV-B: 280–315; UV-A: 315–400; Blue: 420–490; Green: 500–580; Red: 580–700; Far-red: 710–850. The temperature was recorded at 30-min intervals using a HOBO H8 Pro temperature logger (Onset Computer Corporation).

species (*Adenophora triphylla* var. *japonica* and *Prunella vulgaris* L.) in the No-UVB treatment, and one in No-UV/BG treatment (*P. vulgaris* L.) during the experiment.

## 2.4 | Statistical analyses

Linear mixed effect models (LME) were fitted for each leaf trait with spectral treatment as the fixed factor, and species and blocks as random factors, which reduced the effects of plant size and frame position, using the *nlme* package (Pinheiro & Bates, 2000). When the treatment was significant (p < 0.05), further analysis assessed the effects of specific wavelength regions by pairwise contrasts (function *glht*, R package *multcomp*, Hothorn et al., 2008). The contrasts between the spectral treatments: >315 nm versus >280 nm, >400 nm versus >315 nm, >500 nm versus >400 nm, >580 nm versus >500 nm, estimate the effect of UV-B, UV-A, blue light, and green light, respectively. Benjamini-Hochberg (BH)'s method (Benjamini & Hochberg, 1995) was used to correct *p*-values for multiple comparisons. Linear least squares method was used to analyze the correlations among leaf morphological and chemical traits. Extra sum-of-squares F test was used to test whether slopes and intercepts were significantly different. The Box–Cox transformation was applied where appropriate to ensure the normality of response variables (Yeo & Johnson, 2000). In addition, the present experiment pre-included three shade-tolerant species. However, we found that the robustness of the relationships between LMA and functional traits was very weak for shade-tolerant species. Finally, we removed this data and use those of shade-intolerant species only.

3 | RESULTS

3.1 | Spectral-attenuation treatments lead to variation in leaf traits

In the experiment, we firstly measured the 13 leaf traits covering a wide range of variation across the 11 studied species (Table 1) and observed differences of between 1.2 and 9.6 times among species. Across all species in general, LMA and LD were significantly affected by our solar spectral-attenuation treatments (Figure 1; Figures S3 and S4), despite receiving equivalent PAR and temperature (Figure S2). Contrast comparisons found that LMA was significantly reduced by the attenuation of UV-B radiation (by 6.7%) and green light (by 5.9%) (Figure 1A), whereas LD significantly decreased and increased when either UV-A radiation and blue light were attenuated, respectively (Figure 1B).

In terms of chemical traits on a dry-mass basis, concentrations of C, N, and total phenolics were significantly reduced by the attenuation of blue light (Figure S4A–C), while concentrations of C and total phenolics also decreased when green light and UV-B radiation were attenuated, respectively. Lignin concentration was significantly increased by the attenuation of UV-B radiation (Figure S4D).
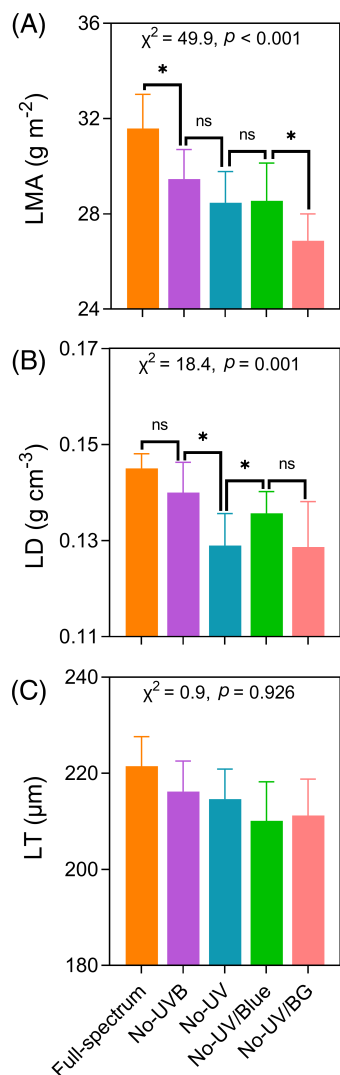
FIGURE 1 Variation in (A) leaf mass per area (LMA), (B) leaf density (LD), and (C) leaf thickness (LT) under different spectral irradiance treatments. Each point represents the mean ± 1 SE trait value of the individuals of each treatment; $n = 9–11$ replicates (one replicate being one plant with 1 measure per plant). Data were analyzed using linear mixed effect models (LME), including treatments as fixed factors, and species and blocks as random factors. Treatment effect is shown by χ^2 and p values. The specific effect of each spectral region is given by contrast comparison between pairs of treatments. *Statistically significant difference ($p < 0.05$) and ns represents no significant difference ($p > 0.05$), tested by Benjamini-Hochberg (BH)'s method

Concentrations of tannins, NSCs, and total soluble sugars were significantly reduced by the attenuation of green light (Figure S4E–G), whereas total soluble sugars also increased when UV-B radiation was attenuated. Starch concentration significantly decreased with the attenuation of UV-A radiation (Figure S4H). These traits on an area basis tended to decrease consistently from Full-spectrum to No-UV/BG treatment; concentrations of most macroelements and metabolites (all except for NSC and starch) were significantly reduced by the attenuation of green light (Figure S5).

3.2 | Relationships between leaf traits among spectral-attenuation treatments

LMA was positively correlated with LD across spectral treatments with similar slopes ($R^2 = 0.48–0.62$, $p < 0.05$, Table S1, Figure 2A), but not with LT; except for one negative relationship from the No-UV treatment ($R^2 = -0.48$, $p = 0.02$, Figure 2B). There were no significant relationships between either of the two components (LD and LT) of LMA, irrespective of spectral treatment (Figure 2C).

LMA was positively correlated with the concentrations of C, N, and total phenolics on a dry-mass basis ($R^2 = 0.09–0.31$, $p < 0.05$, Table S1, Figure 3A), but negatively correlated with the concentrations of lignin, NSCs, and total soluble sugars ($R^2 = -0.20–-0.14$, $p < 0.05$) across all treatments. Regarding each spectral treatment, LMA was positively related with C concentration in the Full-spectrum, No-UVB, and No-UV/BG treatments ($R^2 = 0.46–0.66$, $p < 0.05$), and with N concentration in the Full-spectrum, No-UV/Blue, and No-UV/BG treatments ($R^2 = 0.36–0.69$, $p < 0.05$).

As a whole, LD was also positively correlated with the concentration of total phenolics ($R^2 = 0.08$, $p = 0.04$, Table S1, Figure 3B), and negatively with concentrations of lignin, NSCs, and total soluble sugars ($R^2 = -0.09–-0.29$, $p < 0.05$). Significant relationships of LD with NSCs and total soluble sugars at the treatment level were detected in the No-UVB and No-UV/BG treatments. However, there were no relationships of LD with C or N concentration ($p > 0.05$).

LT was negatively correlated with the concentrations of C, N, and tannin ($R^2 = -0.30–-0.10$, $p < 0.05$, Table S1, Figure 3C) across all treatments. Specifically, LT had negative relationships with N concentration in the Full-spectrum, No-UVB, and No-UV treatments ($R^2 = -0.53–-0.36$, $p < 0.05$), and with tannins in the Full-spectrum and No-UVB treatments ($R^2 = -0.53–-0.41$, $p < 0.05$).

These relationships in each treatment were weak on an area basis (except for those with total soluble sugars, Table S2), whereas LMA and LT were generally positively correlated with C and N for the pooled data, and negatively with other metabolites and structural traits.

4 | DISCUSSION

4.1 | Solar spectral regions determining LMA and its components

We found that LMA significantly decreased when UV-B radiation was attenuated (Figure 1A). Such a UV-B effect is congruent with most previous findings of irradiance dose–response studies because high global irradiance almost always coincided with high UV-B irradiance in the field. For instance, LMA is generally higher across scales of leaves and species that grow in "high light" environments, that is, higher in shade-intolerant than shade-tolerant herb and woody species (Niinemets, 1997; Zhang et al., 2019), and for leaves at the canopy top than those within the canopy (Coble & Cavaleri, 2014, 2015). High UV-B irradiance not only promotes the accumulation of specific phenolic compounds in epidermal tissues (also see Figure S4C) that act as
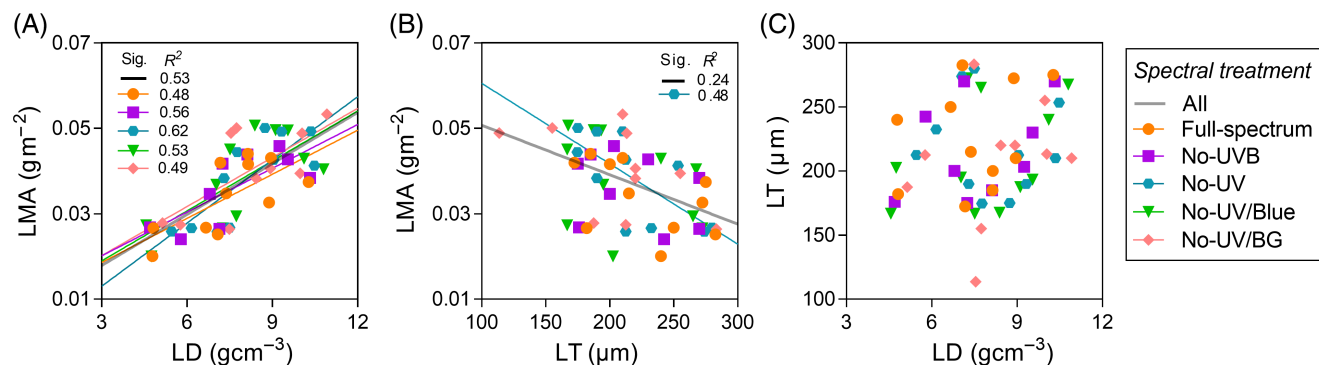
FIGURE 2 Relationship between (A) leaf mass per area (LMA) with leaf density (LD), (B) LMA with leaf thickness (LT), and between (C) LT with LD across species for each spectral treatment. LMA and LD values were transformed by the box–cox power transformation. Solid colored lines denote significant relationships ($p < 0.05$), tested by linear least squares method. R^2 values of the significant relationships were shown next to the respective legend markers. Detailed statistical analyses coefficient and p values are in Table S1
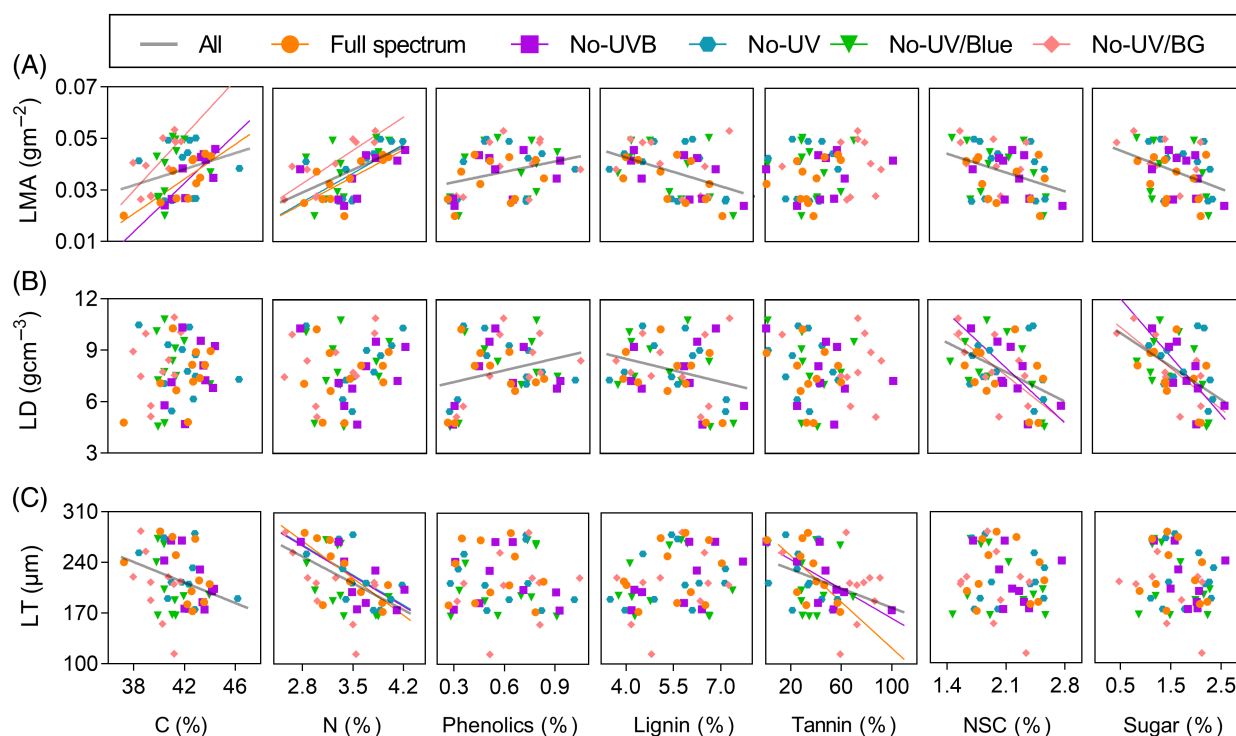
FIGURE 3 Relationship between (A) leaf mass per area (LMA), (B) leaf density (LD), and (C) LMA with leaf chemical concentrations across species for each spectral treatment. Values of LMA, LD, phenolics, tannins, sugars, starch, and non-structure carbohydrates (NSC) were transformed by the box–cox power transformation. Solid colored lines denote significant relationships ($p < 0.05$), tested by linear least squares method. Detailed coefficient and P values are in Table S1. C, carbon; N, nitrogen

UV-absorbing sunscreens (Åke et al., 1994), but also increases LMA to improve UV tolerance, that is, through denser and more compact leaves (Berli et al., 2012). Recent mechanistic studies have revealed that these UV-B responses are regulated by photomorphogenesis mediated by UVR8 (Hayes et al., 2014; Jenkins, 2017; Rizzini et al., 2011). However, a meta-analysis study has not detected a consistent response of LMA to high UV-B irradiance across species of different functional groups and ecosystem types (Poorter et al., 2009), probably due to insufficient data from controlled experiments rather than field monitoring, or maybe

because so many ubiquitous environmental drivers (e.g., temperature and moisture) interact strongly with sunlight to shape LMA (Wang, Liu, et al., 2018).

Interestingly, in addition to indicators of "high light" like UV-B radiation, green light also significantly increased LMA in our experiment from the comparison between No-UV/Blue and No-UV/BG treatments (Figure 1A). Molecular and horticulture studies find that green light generally causes two distinct photomorphogenic effects. It can act as a 'shade' cue antagonistically to blue light, promoting a

more shade-acclimated phenotype (Smith et al., 2017; Zhang et al., 2011). Green light can penetrate deeper into the mesophyll layer than blue and red light (Terashima et al., 2009) and contributes a significant proportion of photosynthetic C assimilation in deeper leaf tissues (Smith et al., 2017). This latter mechanism may explain the change in LMA under green light found in our study, which requires clarification through further specific studies.

Regarding the components of LMA, LD rather than LT significantly responded to our spectral treatments, each of which decreased and increased with the attenuation of UV-A and blue light, respectively (Figure 1B,C). This trend implies that mass allocation or investment within the leaf is more plastic than leaf structure to the changes in spectral composition. Higher LD may reflect smaller cells with thicker cell walls (Garnier & Laurent, 1994), lower volume of airspaces (Coble & Cavaleri, 2017), and a higher proportion of sclerified tissues (Niinemets, 2001). Such "sun-leaf type" characteristics may be mediated by UV-A radiation (Verdaguer et al., 2017), which is perceived by UVR8 (Casati et al., 2011; Rai et al., 2019) and CRYs (Casal, 2013). Both photoreceptors can regulate light acclimation, for example, through an increase in palisade cells and photoprotective pigments. However, it is not clear why blue light rather reduced LD in our experiment (Figure 1B). One possible interpretation is that blue light generally stimulates an increase in stomatal conductance (Hogewoning et al., 2010; Terfa et al., 2013), which may also result in a high proportion of leaf internal air space, consequently contributing to a low LD.

4.2 | Variation in LD explains changes in LMA in response to spectral composition

LMA positively correlated with LD across all spectral treatments (Figure 2A), whereas it negatively correlated with LT only in the treatment where UV radiation was attenuated (Figure 2B). These results suggest that the dependency of LMA on LD is consistent across multiple spectral compositions and inherent among our studied species. This conclusion agrees with previous findings, for example, that LD is a better driver of LMA than LT among 769 native herbs in the field (Wilson et al., 1999) and 14 grasses in the growth room (Garnier & Laurent, 1994). However, all three metrics (LMA, LD, and LT) significantly increase with the rise in solar irradiance from the understorey to canopy top to the forest canopy (Coble & Cavaleri, 2014, 2015; Zhang et al., 2019). These patterns imply that the dependency of LMA on LD may be determined by spectral composition (light quality), but that the strength of irradiance (light intensity) mediates how both LD and LT affect LMA.

This dissociation between the effects of the sunlight intensity and its composition is permitted by the independent relationship between LD and LT (Figure 2C). Earlier studies have also found LD and LT to respond independently to environmental conditions (Kitajima & Poorter, 2010; Niinemets, 1999), with LT generally greater under stress conditions, such as high light, drought, and low temperature (Poorter et al., 2009; Poorter et al., 2019). Higher LT implies that

a greater fraction of leaf tissues is allocated to the mesophyll (Sancho-Knapik et al., 2020), especially in palisade layer, which maximizes overall absorption (Coble & Cavaleri, 2017). Thus, increased LT together with higher LD under strong irradiance would contribute to greater net C assimilation rate and shorten the "leaf pay-back time" (Niinemets, 2001; Poorter et al., 2019). Under the low irradiance, however, high LMA and LD may be advantageous at the expense of short-term C gain (Kitajima, 1994; Valladares & Niinemets, 2008), since increased LD is associated with a decrease in assimilative compounds and modifications in leaf anatomy (Niinemets, 1999).

4.3 | The relationship between leaf morphology and leaf chemical compositions

Based on relationships of LD and LT with leaf chemical compositions, we could understand the allocation strategy in structural components and metabolically functional components when plants receive different spectral compositions. LMA and leaf chemical composition covaried according to the spectral composition of growing conditions (Table S1). LMA was positively correlated with C and N concentration across multiple spectral treatments (Figure 3A), confirming that higher LMA is related to a higher fraction of C in structural tissues (de la Riva et al., 2018) and of N in physiological functioning. Such results seem not support the trade-off in investment between mechanical support and physiological activity, according to the leaf economics spectrum theory (Wright et al., 2004). This expectation is based on the hypothesis that higher C and N allocation to cell walls results in higher mechanical resistance, while the decrease in N to photosynthetic proteins reduces photosynthesis (Onoda et al., 2017). However, the cell wall represents only one aspect of leaf mechanical properties, which also include, for example, cuticle, fibers, and veins (Onoda et al., 2011), while the fraction of N allocated to the cell wall and proteins also varies among species (Onoda et al., 2017). In other words, it is not a given that a higher cell wall fraction leads to less N allocated to photosynthetic apparatus. This possibility is supported by a study that found leaf mechanical strength to vary independently from photosynthetic capacity across 57 shade-tolerant and light-demanding species (He et al., 2019).

As a whole, LMA and LD were negatively correlated with mass-based concentrations of lignin, NSCs, and sugars (Figure 3A,B). This relationship indicates a trade-off between LMA and metabolite accumulation per leaf mass, which may be the result of greater mass allocation to structural components than metabolically functional components (those contribute to improve stress tolerance) with a high LMA (Li et al., 2013). Notably, LMA and LD were positively correlated with mass-based concentrations of total phenolics (Figure 3A,B), the dominant compounds of stress tolerance. Phenolics are C-rich compounds (ca. 30% C on a mass basis) compared with proteins (Poorter, 1994), and their accumulation in leaf vacuoles and cell walls can increase LD (Witkowski & Lamont, 1991). In addition, these dependencies of LMA on metabolite composition were less differentiated among spectral treatments (Figure 3A, Table S1), perhaps due to

the overlapping action spectra of photoreceptors. It is known that the synthesis of specialized (secondary) metabolites is generally mediated by multiple wavelength regions (Casal, 2013; Casal & Qüesta, 2018; Robson et al., 2015; Smith et al., 2017; Verdaguer et al., 2017). Their combined effects would be synergistic, additive, or antagonistic when plants simultaneously receive light from multiple regions (Rai et al., 2019; Wang et al., 2020). Nevertheless, the relationships discussed above need to be confirmed in more species, since the present experiment just used 11 species, which may limit the robustness.

5 | CONCLUSIONS

The present study demonstrates that LMA and its morphological components, and leaf elemental and metabolite compositions varied significantly in response to solar spectral composition across 11 forb species in spectral attenuation treatments receiving the same PAR irradiance. LMA variation was determined by UV-B radiation and green light, and in general was mainly dependent on LD rather than LT. Changes in leaf elemental and metabolic composition, on the mass-basis, under our spectral attenuation treatments were associated with changes in LMA, which implies a trade-off in biomass allocation between structural and metabolically functional components. These results suggest that the spectral composition of solar radiation can regulate LMA irrespective of total irradiance by modifying mass investment and structural support.

AUTHOR CONTRIBUTIONS

Qing-Wei Wang, Hiroko Kurokawa, and Thomas Matthew Robson conceived and designed the experiment; Qing-Wei Wang carried out the growth experiment and performed most trait measurements; Chenggang Liu determined concentrations of leaf total soluble sugars and starch; Qing-Wei Wang provided statistical analysis; Qing-Wei Wang wrote the draft of the manuscript; and Kouki Hikosaka, Thomas Matthew Robson, Hiroko Kurokawa, and Chenggang Liu revised the manuscript.

ORCID

Qing-Wei Wang https://orcid.org/0000-0002-5169-9881
Chenggang Liu https://orcid.org/0000-0002-4366-1429
Thomas Matthew Robson https://orcid.org/0000-0002-8631-796X
Kouki Hikosaka https://orcid.org/0000-0003-1744-3775
Hiroko Kurokawa https://orcid.org/0000-0001-8778-8045

REFERENCES

Adler, P.B., Salguero-Gomez, R., Compagnoni, A., Hsu, J.S., Ray-Mukherjee, J., Mbeau-Ache, C. et al. (2014) Functional traits explain variation in plant life history strategies. *Proceedings of the National Academy of Sciences of the United States of America*, 111(2), 740–745.

Åke, S., Chow, W.S. & Anderson, J.M. (1994) UV-B damage and protection at the molecular level in plants. *Photosynthesis Research*, 39, 475–489.

Aphalo, P.J. & Lehto, T. (2001) Effect of lateral far-red light supplementation on the growth and morphology of birch seedlings and its interaction with mineral nutrition. *Trees*, 15(5), 297–303.

Ballaré, C.L. (2014) Light regulation of plant defense. *Annual Review of Plant Biology*, 65, 335–363.

Benjamini, Y. & Hochberg, Y. (1995) Controlling the false discovery rate: a practical and powerful approach to multiple testing. *Journal of the Royal Statistical Society Series B (Methodological)*, 57, 289–300.

Berli, F.J., Alonso, R., Bressan-Smith, R. & Bottini, R. (2012) UV-B impairs growth and gas exchange in grapevines grown in high altitude. *Physiologia Plantarum*, 149(1), 127–140.

Brelsford, C.C., Morales, L.O., Nezval, J., Kotilainen, T.K., Hartikainen, S.M., Aphalo, P.J. et al. (2019) Do UV-A radiation and blue light during growth prime leaves to cope with acute high light in photoreceptor mutants of *Arabidopsis thaliana*? *Physiologia Plantarum*, 165(3), 537–554.

Casal, J.J. (2000) Phytochromes, cryptochromes, phototropin: photoreceptor interactions in plants. *Photochemistry and Photobiology*, 71(1), 1–11.

Casal, J.J. (2013) Photoreceptor signaling networks in plant responses to shade. *The Annual Review of Plant Biology*, 64, 403–427.

Casal, J.J. & Qüesta, J.I. (2018) Light and temperature cues: multitasking receptors and transcriptional integrators. *New Phytologist*, 217(3), 1029–1034.

Casati, P., Campi, M., Morrow, D.J., Fernandes, J.F. & Walbot, V. (2011) Transcriptomic, proteomic and metabolomic analysis of UV-B signaling in maize. *BMC Genomics*, 12(1), 321.

Coble, A.P. & Cavaleri, M.A. (2014) Light drives vertical gradients of leaf morphology in a sugar maple (*Acer saccharum*) forest. *Tree Physiology*, 34(2), 146–158.

Coble, A.P. & Cavaleri, M.A. (2015) Light acclimation optimizes leaf functional traits despite height-related constraints in a canopy shading experiment. *Oecologia*, 177(4), 1131–1143.

Coble, A.P. & Cavaleri, M.A. (2017) Vertical leaf mass per area gradient of mature sugar maple reflects both height-driven increases in vascular tissue and light-driven increases in palisade layer thickness. *Tree Physiology*, 37(10), 1337–1351.

Cornwell, W.K., Cornelissen, J.H., Amatangelo, K., Dorrepaal, E., Eviner, V.T., Godoy, O. et al. (2008) Plant species traits are the predominant control on litter decomposition rates within biomes worldwide. *Ecology Letters*, 11(10), 1065–1071.

Duursma, R.A. & Falster, D.S. (2016) Leaf mass per area, not total leaf area, drives differences in above-ground biomass distribution among woody plant functional types. *New Phytologist*, 212(2), 368–376.

Fajardo, A. & Piper, F.I. (2011) Intraspecific trait variation and covariation in a widespread tree species (Nothofagus pumilio) in southern Chile. *New Phytologist*, 189(1), 259–271.

Fajardo, A. & Siefert, A. (2016) Temperate rain forest species partition fine-scale gradients in light availability based on their leaf mass per area (LMA). *Annals of Botany*, 118(7), 1307–1315.

Fernandez-Martinez, J., Fransi, M.A. & Fleck, I. (2016) Ecophysiological responses of *Betula pendula*, Pinus uncinata and *Rhododendron ferrugineum* in the Catalan Pyrenees to low summer rainfall. *Tree Physiology*, 36(12), 1520–1535.

Fukushima, R.S. & Hatfield, R.D. (2001) Extraction and isolation of lignin for utilization as a standard to determine lignin concentration using the acetyl bromide spectrophotometric method. *Journal of Agricultural and Food Chemistry*, 49(7), 3133–3139.

Garnier, E. & Laurent, G. (1994) Leaf anatomy, specific mass and water content in congeneric annual and perennial grass species. *New Phytologist*, 128(4), 725–736.

Griffith, D.M., Quigley, K.M. & Anderson, T.M. (2016) Leaf thickness controls variation in leaf mass per area (LMA) among grazing-adapted grasses in Serengeti. *Oecologia*, 181(4), 1035–1040.

Hartikainen, S.M., Jach, A., Grané, A. & Robson, T.M. (2018) Assessing scale-wise similarity of curves with a thick pen: as illustrated through comparisons of spectral irradiance. *Joural Ecology and Evolution*, 8(20), 10206–10218.

Hayes, S., Velanis, C.N., Jenkins, G.I. & Franklin, K.A. (2014) UV-B detected by the UVR8 photoreceptor antagonizes auxin signaling and plant shade avoidance. *Proceedings of the National Academy of Sciences of the United States of America*, 111(32), 11894–11899.

He, P., Wright, I.J., Zhu, S., Onoda, Y., Liu, H., Li, R. et al. (2019) Leaf mechanical strength and photosynthetic capacity vary independently across 57 subtropical forest species with contrasting light requirements. *New Phytologist*, 223(2), 607–618.

Hikosaka, K., Terashima, I. & Katoh, S. (1994) Effects of leaf age, nitrogen nutrition and photon flux density on the distribution of nitrogen among leaves of a vine (*Ipomoea tricolor* Cav.) grown horizontally to avoid mutual shading of leaves. *Oecologia*, 97, 451–457.

Hikosaka, K., Onoda, Y., Kinugasa, T., Nagashima, H., Anten, N.P.R. & Hirose, T. (2005) Plant responses to elevated CO_2 concentration at different scales: leaf, whole plant, canopy, and population. *Ecological Research*, 20(3), 243–253.

Hogewoning, S.W., Trouwborst, G., Maljaars, H., Poorter, H., van Ieperen, W. & Harbinson, J. (2010) Blue light dose-responses of leaf photosynthesis, morphology, and chemical composition of *Cucumis sativus* grown under different combinations of red and blue light. *Journal of Experimental Botany*, 61(11), 3107–3117.

Hothorn, T., Bretz, F. & Westfall, P. (2008) Simultaneous inference in general parametric models. *Biometrical Journal*, 50(3), 346–363.

Hu, J., Dai, X. & Sun, G. (2016) Morphological and physiological responses of morus alba seedlings under different light qualities. *Notulae Botanicae Horti Agrobotanici Cluj-Napoca*, 44(2), 382–392.

Iiyama, K. & Wallis, A.F. (1990) Determination of lignin in herbaceous plants by an improved acetyl bromide procedure. *Journal of the Science of Food and Agriculture*, 51(2), 145–161.

Ishizaki, S., Hikosaka, K. & Hirose, T. (2003) Increase in leaf mass per area benefits plant growth at elevated CO_2 concentration. *Annals of Botany*, 91(7), 905–914.

Jenkins, G.I. (2017) Photomorphogenic responses to ultraviolet-B light. *Plant, Cell & Environment*, 40(11), 2544–2557.

Jenkins, G.I., Long, J.C., Wade, H.K., Shenton, M.R. & Bibikova, T.N. (2001) UV and blue light signalling: pathways regulating chalcone synthase gene expression in Arabidopsis. *New Phytologist*, 151(1), 121–131.

John, G.P., Scoffoni, C., Buckley, T.N., Villar, R., Poorter, H. & Sack, L. (2017) The anatomical and compositional basis of leaf mass per area. *Ecology Letters*, 20(4), 412–425.

Julkunen-Tiitto, R. (1985) Phenolic constituents in the leaves of northern willows: methods for the analysis of certain phenolics. *Journal of Agricultural and Food Chemistry*, 33(2), 213–217.

Kitajima, K. (1994) Relative importance of photosynthetic traits and allocation patterns as correlates of seedling shade tolerance of 13 tropical trees. *Oecologia*, 98(3–4), 419–428.

Kitajima, K. & Poorter, L. (2010) Tissue-level leaf toughness, but not lamina thickness, predicts sapling leaf lifespan and shade tolerance of tropical tree species. *The New Phytologist*, 186(3), 708–721.

Li, Y., Yang, D.M., Xiang, S. & Li, G.Y. (2013) Different responses in leaf pigments and leaf mass per area to altitude between evergreen and deciduous woody species. *Australian Journal of Botany*, 61(6), 424–435.

Lin, C. (2000) Plant blue-light receptors. *Trends in Plant Science*, 5(8), 337–342.

Liu, Y., Wang, T.L., Fang, S.Z., Zhou, M.M. & Qin, J. (2018) Responses of morphology, gas exchange, photochemical activity of photosystem II, and antioxidant balance in *Cyclocarya paliurus* to light spectra. *Frontiers in Plant Science*, 9, 1704.

Moss, D.N. (1967) Solar energy in photosynthesis. *Solar Energy*, 11(3–4), 173–179.

Niinemets, U. (1997) Role of foliar nitrogen in light harvesting and shade tolerance of four temperate deciduous woody species. *Functional Ecology*, 11(4), 518–531.

Niinemets, U. (1999) Components of leaf dry mass per area – thickness and density – alter leaf photosynthetic capacity in reverse directions in woody plants. *New Phytologist*, 144(1), 35–47.

Niinemets, U. (2001) Global-scale climatic controls of leaf dry mass per area, density, and thickness in trees and shrubs. *Ecology*, 82(2), 453–469.

Oguchi, R., Hikosaka, K. & Hirose, T. (2005) Leaf anatomy as a constraint for photosynthetic acclimation: differential responses in leaf anatomy to increasing growth irradiance among three deciduous trees. *Plant, Cell & Environment*, 28(7), 916–927.

Oguchi, R., Hiura, T. & Hikosaka, K. (2017) The effect of interspecific variation in photosynthetic plasticity on 4-year growth rate and 8-year survival of understorey tree seedlings in response to gap formations in a cool-temperate deciduous forest. *Tree Physiology*, 37(8), 1113–1127.

O'Hara, A., Headland, L.R., Díaz-Ramos, L.A., Morales, L.O., Strid, Å. & Jenkins, G.I. (2019) Regulation of Arabidopsis gene expression by low fluence rate UV-B independently of UVR8 and stress signaling. *Photochemical & Photobiological Sciences*, 18, 1675–1684.

Onoda, Y., Schieving, F. & Anten, N.P.R. (2008) Effects of light and nutrient availability on leaf mechanical properties of *Plantago major*: a conceptual approach. *Annals of Botany*, 101(5), 727–736.

Onoda, Y., Westoby, M., Adler, P.B., Choong, A.M., Clissold, F.J., Cornelissen, J.H. et al. (2011) Global patterns of leaf mechanical properties. *Ecology Letters*, 14(3), 301–312.

Onoda, Y., Wright, I.J., Evans, J.R., Hikosaka, K., Kitajima, K., Niinemets, Ü. et al. (2017) Physiological and structural tradeoffs underlying the leaf economics spectrum. *New Phytologist*, 214(4), 1447–1463.

Peeters, P.J. (2002) Correlations between leaf structural traits and the densities of herbivorous insect guilds. *Biological Journal of the Linnean Society*, 77(1), 43–65.

Pinheiro, J.C. & Bates, D.M. (2000) Linear mixed-effects models: basic concepts and examples. *Mixed-Effects Models in Sand S-PLUS*. New York, USA: Springer New York, pp. 3–56.

Poorter, H. (1994) Construction costs and payback time of biomass: a whole plant perspective. In: *A whole plant perspective on carbon-nitrogen interactions*. The Hague, The Netherland: SPB Academic Publishing bv, pp. 111–127.

Poorter, H. & Villar, R. (1997) *Chemical composition of plants: causes and consequences of variation in allocation of C to different plant constituents*. New York: Plant Resource Allocation Academic Press, pp. 39–72.

Poorter, H., Niinemets, Ü., Poorter, L., Wright, I.J. & Villar, R. (2009) Causes and consequences of variation in leaf mass per area (LMA): a meta-analysis. *New Phytologist*, 182(3), 565–588.

Poorter, H., Niinemets, U., Ntagkas, N., Siebenkas, A., Maenpaa, M., Matsubara, S. et al. (2019) A meta-analysis of plant responses to light intensity for 70 traits ranging from molecules to whole plant performance. *The New Phytologist*, 223, 1073–1105.

Rai, N., Neugart, S., Yan, Y., Wang, F., Siipola, S.M., Lindfors, A.V. et al. (2019) How do cryptochromes and UVR8 interact in natural and simulated sunlight? *Journal of Experimental Botany*, 70, 4975–4990.

Razzak, A., Ranade, S.S., Strand, A. & Garcia-Gil, M.R. (2017) Differential response of Scots pine seedlings to variable intensity and ratio of red and far-red light. *Plant, Cell & Environment*, 40(8), 1332–1340.

Reich, P.B., Walters, M.B. & Ellsworth, D.S. (1997) From tropics to tundra: global convergence in plant functioning. *Proceedings of the National Academy of Sciences of the United States of America*, 94(25), 13730–11373.

de la Riva, E.G., Olmo, M., Poorter, H., Ubera, J.L. & Villar, R. (2016) Leaf mass per area (LMA) and its relationship with leaf structure and anatomy in 34 Mediterranean woody species along a water availability gradient. *PLoS One*, 11(2), e0148788.

de la Riva, E.G., Villar, R., Perez-Ramos, I.M., Quero, J.L., Matias, L., Poorter, L. et al. (2018) Relationships between leaf mass per area and nutrient concentrations in 98 Mediterranean woody species are determined by phylogeny, habitat and leaf habit. *Trees*, 32(2), 497–510.

Rizzini, L., Favory, J.J., Cloix, C., Faggionato, D., O'Hara, A., Kaiserli, E. et al. (2011) Perception of UV-B by the Arabidopsis UVR8 protein. *Science*, 332(6025), 103–106.

Robson, T.M., Klem, K., Urban, O. & Jansen, M.A. (2015) Re-interpreting plant morphological responses to UV-B radiation. *Plant, Cell and Environment*, 38(5), 856–866.

Robson, T.M., Aphalo, P.J., Banas, A.K., Barnes, P.W., Brelsford, C.C., Jenkins, G.I. et al. (2019) A perspective on ecologically relevant plant-UV research and its practical application. *Photochemical & Photobiological Sciences*, 18, 970–988.

Rousseaux, M.C., Julkunen-Tiitto, R., Searles, P.S., Scopel, A.L., Aphalo, P.J. & Ballare, C.L. (2004) Solar UV-B radiation affects leaf quality and insect herbivory in the southern beech tree Nothofagus Antarctica. *Oecologia*, 138(4), 505–512.

Sanchez-Gomez, D., Robson, T.M., Gasco, A., Gil-Pelegrin, E. & Aranda, I. (2013) Differences in the leaf functional traits of six beech (*Fagus sylvatica* L.) populations are reflected in their response to water limitation. *Environmental and Experimental Botany*, 87, 110–119.

Sancho-Knapik, D., Escudero, A., Mediavilla, S., Scoffoni, C., Zailaa, J., Cavender-Bares, J. et al. (2020) Deciduous and evergreen oaks show contrasting adaptive responses in leaf mass per area across environments. *The New Phytologist*, 230, 521–534.

Searles, P.S., Flint, S.D. & Caldwell, M.M. (2001) A meta analysis of plant field studies simulating stratospheric ozone depletion. *Oecologia*, 127(1), 1–10.

Smith, H. (2000) Phytochromes and light signal perception by plants – an emerging synthesis. *Nature*, 407(6804), 585–591.

Smith, H.L., McAusland, L. & Murchie, E.H. (2017) Don't ignore the green light: exploring diverse roles in plant processes. *Journal of Experimental Botany*, 68(9), 2099–2110.

Terashima, I., Fujita, T., Inoue, T., Chow, W.S. & Oguchi, R. (2009) Green light drives leaf photosynthesis more efficiently than red light in strong white light: revisiting the enigmatic question of why leaves are green. *Plant & Cell Physiology*, 50(4), 684–697 Review.

Terfa, M.T., Solhaug, K.A., Gislerød, H.R., Olsen, J.E. & Torre, S. (2013) A high proportion of blue light increases the photosynthesis capacity and leaf formation rate of Rosa × hybrida but does not affect time to flower opening. *Physiologia Plantarum*, 148(1), 146–159.

Valladares, F. & Niinemets, U. (2008) Shade tolerance, a key plant feature of complex nature and consequences. In: *Annual review of ecology evolution and systematics*. Palo Alto, USA: Annual Reviews, pp. 237–257.

Verdaguer, D., Jansen, M.A., Llorens, L., Morales, L.O. & Neugart, S. (2017) UV-A radiation effects on higher plants: exploring the known unknown. *Plant Science*, 255, 72–81.

Wang, Q.-W., Liu, C.-G., Zhou, W., Qi, L., Zhou, L., Yu, D. et al. (2018) Mobile carbon supply in trees and shrubs at the alpine treeline ecotone. *Plant Ecology*, 219(4), 467–479.

Wang, Q.W., Qi, L., Zhou, W., Liu, C.G., Yu, D. & Dai, L. (2018) Carbon dynamics in the deciduous broadleaf tree Erman's birch (*Betula ermanii*) at the subalpine treeline on Changbai Mountain, Northeast China. *American Journal of Botany*, 105(1), 42–49.

Wang, Q.-W., Daumal, M., Nagano, S., Yoshida, N., Morinaga, S.-I. & Hikosaka, K. (2019) Plasticity of functional traits and optimality of biomass allocation in elevational ecotypes of Arabidopsis halleri grown at different soil nutrient availabilities. *Journal of Plant Research*, 132(2), 237–249.

Wang, Q.-W., Robson, T.M., Pieristè, M., Oguro, M., Oguchi, R., Murai, Y. & Kurokawa, H. (2020) Testing trait plasticity over the range of spectral composition of sunlight in forb species differing in shade tolerance. *Journal of Ecology*, 108(5), 1923–1940.

Waterman, P.G. & Mole, S. (1994) *Analysis of phenolic plant metabolites*. Boston, USA: Blackwell Scientific.

Wilson, P.J., Thompson, K. & Hodgson, J.G. (1999) Specific leaf area and leaf dry matter content as alternative predictors of plant strategies. *New Phytologist*, 143(1), 155–162.

Witkowski, E. & Lamont, B.B. (1991) Leaf specific mass confounds leaf density and thickness. *Oecologia*, 88(4), 486–493.

Wright, I.J., Westoby, M. & Reich, P.B. (2002) Convergence towards higher leaf mass per area in dry and nutrient-poor habitats has different consequences for leaf life span. *Journal of Ecology*, 90(3), 534–543.

Wright, I.J., Reich, P.B., Westoby, M., Ackerly, D.D., Baruch, Z., Bongers, F. et al. (2004) The worldwide leaf economics spectrum. *Nature*, 428(6985), 821–827.

Xu, C.Y., Salih, A., Ghannoum, O. & Tissue, D.T. (2012) Leaf structural characteristics are less important than leaf chemical properties in determining the response of leaf mass per area and photosynthesis of *Eucalyptus saligna* to industrial-age changes in CO_2 and temperature. *Journal of Experimental Botany*, 63(16), 5829–5841.

Yeo, I.K. & Johnson, R.A. (2000) A new family of power transformations to improve normality or symmetry. *Biometrika*, 87(4), 954–959.

Zhang, T., Maruhnich, S.A. & Folta, K.M. (2011) Green light induces shade avoidance symptoms. *Plant Physiology*, 157(3), 1528–1536.

Zhang, X., Jin, G. & Liu, Z. (2019) Contribution of leaf anatomical traits to leaf mass per area among canopy layers for five coexisting broadleaf species across shade tolerances at a regional scale. *Forest Ecology and Management*, 452(15), 117569.

Zhang, L., Yang, L. & Shen, W. (2020) Dramatic altitudinal variations in leaf mass per area of two plant growth forms at extreme heights. *Ecological Indicators*, 110, 105890.

SUPPORTING INFORMATION

Additional supporting information may be found online in the Supporting Information section at the end of this article.